Theor Ecol (2011) 4:13–25
DOI 10.1007/s12080-010-0071-3

ORIGINAL PAPER

Discrete-time growth-dispersal models with shifting species ranges

Ying Zhou · Mark Kot

Received: 26 October 2009 / Accepted: 15 January 2010 / Published online: 2 February 2010

Abstract Many species are responding to global climate change by shifting their ranges poleward in latitude or upward in elevation. We analyze an integrodifference equation that combines growth, dispersal, and a constant-speed, climate-induced range shift and find that a shifting population can die out, even if the width of its range remains constant. We show how to determine the critical range-shift speed (for extinction) and study the effects of the growth rate and of the shape and scale of the dispersal kernel on persistence.

Keywords Climate change · Population persistence · Range shift · Integrodifference equation

Introduction

The Earth's climate is warming. Global average temperatures have increased by 0.13 °C per decade over the last 50 years (1956–2005). Further warming, at an even faster rate, is expected over the next 50 years (IPCC 2007). This warming is expected to cause species to shift their ranges poleward in latitude or upward in elevation (Parmesan et al. 1999; Hughes 2000; McCarty 2001; Walther et al. 2002; Lovejoy and Hannah 2005). Ecologists must now face the challenge of predicting the range-shifting responses of the Earth's biota.

Y. Zhou (✉) · M. Kot
Department of Applied Mathematics,
University of Washington, Seattle, USA
e-mail: yzhou@amath.washington.edu

M. Kot
e-mail: kot@amath.washington.edu

Bioclimate envelope models are commonly used to assess the impacts of climate change on species distributions (Box 1981; Jeffree and Jeffree 1996; Bakkenes et al. 2002; Guisan and Thuiller 2005). These statistical models correlate the current distribution of a species with climatic variables such as degree-days, maximum and minimum temperatures, and water balance. Ideally, scientists can combine a species' climate envelope with projections of climate change to predict a species' new distribution.

The use of bioclimate envelope models has, however, been contentious (Kadmon et al. 2003; Pearson and Dawson 2003). One (of several) criticisms is that bioclimate envelope models do not account for species dispersal (Gaston 2003; Pearson and Dawson 2003; Mitikka et al. 2008). Rather, they predict the *potential* ranges of species. Poor dispersers may, in general, fail to live up to their potential.

Can a species keep pace with climate-induced range shifts? We believe that one must use a mathematical model that incorporates growth, dispersal, and climate-driven spatial shifts to answer this question.

There are many mathematical models that describe the growth and dispersal of biological populations (Kareiva 1990; Keeling 1999; Shigesada and Kawasaki 2002). The use of reaction-diffusion equations (Fisher 1937; Skellam 1951; Okubo 1980; Shigesada and Kawasaki 1997; Cantrell and Cosner 2003) is especially common. For reaction-diffusion models, space and time are continuous. Growth and diffusion, moreover, are assumed to occur simultaneously. Recently, Potapov and Lewis (2004) and Berestycki et al. (2009) used reaction-diffusion models to study the effects of climate change on the ranges of plants and animals. Berestycki et al. (2009), in

particular, showed that if a habitat shifts too rapidly, species may go extinct.

Many species have distinct growth and dispersal stages. Summer annuals, for example, may germinate in spring, flower in summer, and disperse their seeds in autumn. Insects typically disperse as adults, and only less so as larvae (Osborne et al. 2002). For these species, ecologists increasingly use integrodifference equations (Kot and Schaffer 1986; Hastings and Higgins 1994; Neubert et al. 1995; Kot et al. 1996; Van Kirk and Lewis 1997; Latore et al. 1998; Neubert and Caswell 2000; Lockwood et al. 2002; Lewis et al. 2006; Lutscher 2008) instead of reaction-diffusion models. Integrodifference equations are discrete-time, continuous-space models. In the simplest case, with discrete, nonoverlapping generations, one writes

$$n_{t+1}(x) = \int_{\Omega} k(x, y)\, f\big[n_t(y)\big]\, dy. \tag{1}$$

Here, $n_t(x)$ is the population density in generation t at location x, Ω is the spatial domain, $f(n)$ is the recruitment or growth function, and $k(x, y)$ is the redistribution or dispersal kernel.

Integrodifference equations can, because of their protean kernel, handle a diverse assortment of dispersal mechanisms (Neubert et al. 1995). These equations have, as a result, been used for a wide variety of applications. Two of these applications are especially relevant to the current problem. The first application is the study of population persistence (Kot and Schaffer 1986; Van Kirk and Lewis 1997, 1999; Latore et al. 1998, 1999; Lockwood et al. 2002). Latore et al. (1998, 1999), for example, studied persistence on a finite, homogeneous, one-dimensional patch of size or length L using the integrodifference equation

$$n_{t+1}(x) = \int_{-\frac{L}{2}}^{\frac{L}{2}} k(x, y)\, f\big[n_t(y)\big]\, dy. \tag{2}$$

Since individuals disperse and are lost across patch boundaries, there is a critical patch size below which the patch's population cannot persist. This critical size depends on both the population's growth rate and on the kernel $k(x, y)$, which implicitly defines the boundary conditions.

The other application is the study of invasive organisms (Kot et al. 1996; Neubert and Caswell 2000; Neubert and Parker 2004; Fagan et al. 2005; Lewis et al. 2006). These studies typically start with an integrodifference equation on an infinite domain,

$$n_{t+1}(x) = \int_{-\infty}^{\infty} k(x, y)\, f\big[n_t(y)\big]\, dy. \tag{3}$$

Integrodifference equations can, like reaction-diffusion equations, generate constant-speed traveling waves (Weinberger 1978, 1982; Lui 1983; Kot 1992; Hart and Gardner 1997). They may, however, also generate accelerating invasions (Kot et al. 1996; Lewis 1997; Clark 1998).

The problem we consider involves both population persistence and invasion. We examine an integrodifference equation in which all growth occurs on a finite domain that moves at a constant speed, mimicking a climate-driven range shift. (In future work, we also hope to examine accelerating range shifts.) Warming may, of course, affect different parts of the life cycle. In this paper, we focus on the impact of warming on reproductive processes because of the demonstrated effect of climate change on phenology and reproductive biology (Gaston 2003; McCarty 2001; Walther et al. 2002; Parmesan 2006; Letcher 2009). We do not, in contrast, consider direct effects of warming on dispersal since this is thought to be less important (but see "Application").

In the next section, we describe our model in detail, provide mathematical background, and give a numerical example of how the speed with which a patch shifts affects persistence. The "Analysis of population persistence" section contains mathematical analyses that explain the phenomena observed in "Model" section. "A simple, separable example" and "Numerical methods" sections focus on analytically and numerically tractable examples. In the "Application" section, we illustrate our ideas using data for Fender's blue butterfly (*Icaricia icarioides fenderi*), an endangered subspecies of Oregon's Willamette Valley (Schultz et al. 2003). Finally, the "Discussion" section contains our discussion and concluding remarks.

Model

We begin by considering the integrodifference equation

$$n_{t+1}(x) = \int_{-\frac{L}{2}+ct}^{\frac{L}{2}+ct} k(x, y)\, f\big[n_t(y)\big]\, dy. \tag{4}$$

This equation differs from a model on a stationary domain, Eq. 2, in its limits of integration, and hence, its habitat boundaries. Our population is no longer restricted to an immobile one-dimensional patch. Rather, our population reproduces on an interval, initially $[-L/2, L/2]$, that moves, because of climate change, to the right, at constant speed c. We will use this

formulation for both latitudinal and elevational range shifts.

Equation 4 maps the density of the population in generation t, $n_t(x)$, $x \in (-\infty, \infty)$, to the density in the next generation, $n_{t+1}(x)$, in two stages. The first stage accounts for the sedentary part of the organism's life cycle. During this stage, individuals inside the interval $[-(L/2) + ct, (L/2) + ct]$ grow, reproduce, and die. The local density inside the interval, $n_t(x)$, is replaced by a new density, $f[n_t(x)]$, of propagules. Individuals outside the interval fail to reproduce.

The function f is the growth or recruitment function. Well-known choices for f include the right-hand sides of the Beverton–Holt (1957) stock-recruitment curve,

$$n_{t+1} = \frac{R_0 n_t}{1 + [(R_0 - 1)/K] n_t}, \tag{5}$$

the logistic difference equation (Maynard Smith 1968; May 1973),

$$n_{t+1} = (1 + r) n_t - \frac{r}{K} n_t^2, \tag{6}$$

and the Ricker (1954) curve,

$$n_{t+1} = n_t e^{r(1 - \frac{n_t}{K})}. \tag{7}$$

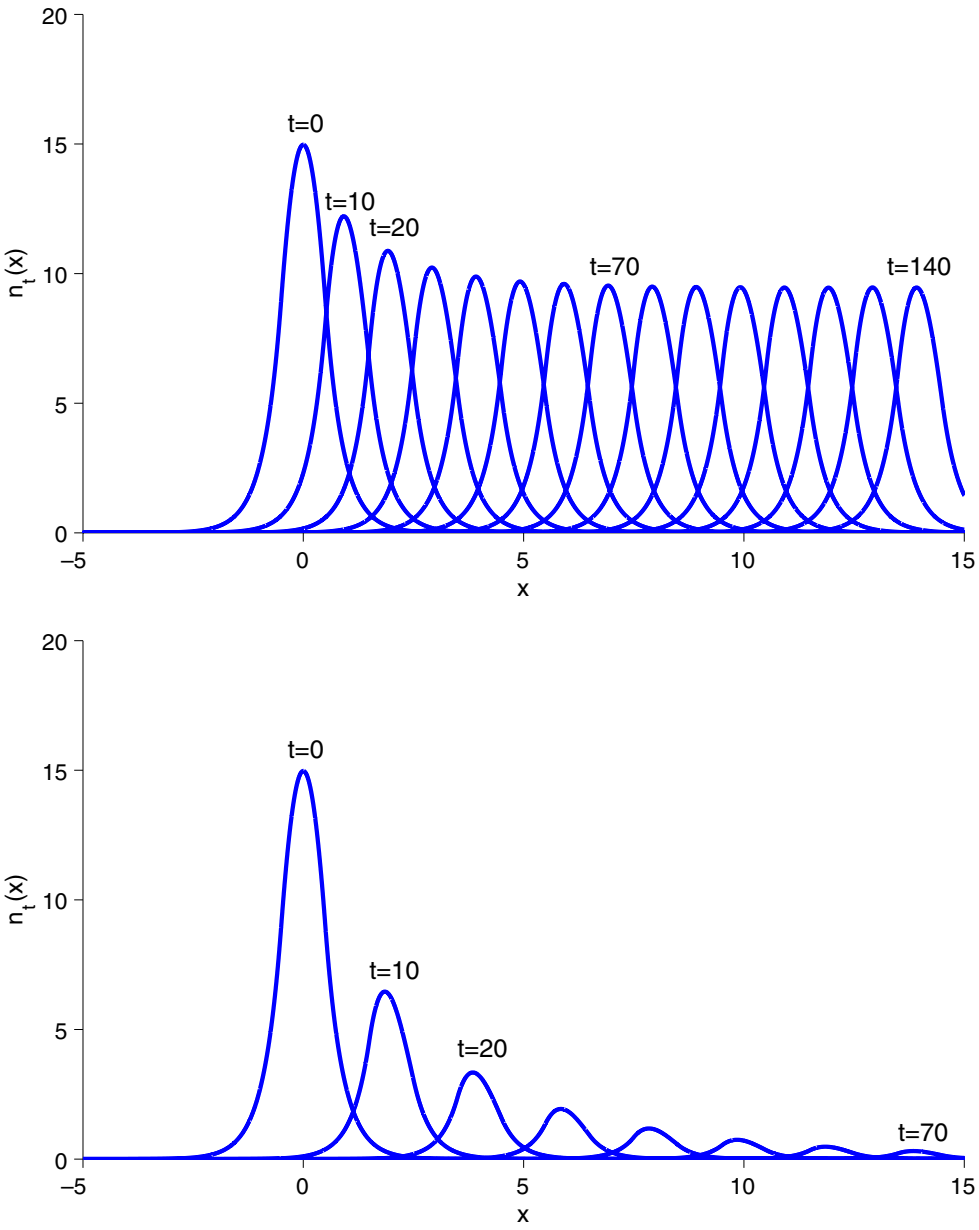

Fig. 1 Simulations of the distribution of a population on a one-dimensional patch of size $L = 1$ show that the population will die out when the speed c is large. For this simulation, we used Laplace dispersal kernel (10), with $b = 2.5$, and Beverton–Holt stock-recruitment curve (5), with $R_0 = 1.7$ and $K = 100$. The initial distribution, marked $t = 0$, was obtained by iterating convolution equation (9), with $c = 0$, for a point release of 50 individuals at $x = 0$ for 120 generations, so that the population converged to a steady distribution. We then iterated Eq. 9 with **a** $c = 0.1$ and **b** $c = 0.2$. In **a**, the population persisted. In **b**, the population went extinct. The distribution is displayed every ten generations and was computed using an FFT-assisted implementation of the extended trapezoidal rule with 2^{16} nodes

Here, K is the carrying capacity of the environment, R_0 is the net reproductive rate, and r is the intrinsic rate of growth. In this paper, we only consider nonnegative growth functions that satisfy

$$f(n) \leq f'(0)\, n. \tag{8}$$

That is, we explicitly exclude growth functions with Allee (1938) effects.

In the second (or dispersal) stage, propagules disseminate. This movement is described by the dispersal kernel $k(x, y)$. For a fixed source y, we may think of the kernel as the probability density function for the destination, x, of the propagules. In this paper, we consider dispersal to be homogeneous and isotropic. We thus assume that our dispersal kernel is both a difference kernel, $k(x, y) = k(x - y)$, and symmetric. Equation 4 can now be written as the convolution equation

$$n_{t+1}(x) = \int_{-\frac{L}{2}+ct}^{\frac{L}{2}+ct} k(x-y)\; f\big[n_t(y)\big]\, dy. \tag{9}$$

Our difference kernel acts as a probability density function for the displacement of the propagules. Well-known examples of symmetric difference kernels include the Gaussian, Laplace, and Cauchy distributions. The convolution integral tallies all propagules within the shifted patch $[-(L/2) + ct, (L/2) + ct]$ that have x as their final destination.

The presence of a shifting or moving range can have a profound effect on the dynamics of a population. Figure 1 shows that an increase in the speed c can cause extinction. This figure was obtained by simulating Eq. 9 with the Laplace kernel,

$$k(x-y) = \frac{1}{2}\, b\; \exp\left(-b\,|x-y|\right), \tag{10}$$

and the Beverton–Holt stock-recruitment curve, Eq. 5. For $L = 1$, $b = 2.5$, $R_0 = 1.7$, $K = 100$, and a small speed of translation ($c = 0.1$), the population persists (Fig. 1a). When we increase the speed to $c = 0.2$, however, the population cannot keep up with climate change and goes extinct (Fig. 1b). Berestycki et al. (2009) observed similar events for their reaction-diffusion model.

Our simulations suggest that there is an upper limit on the speed, $c = c^*$, with which a population can move. Beyond this critical speed, a population cannot persist unless other parameters also change. Increasing the net reproductive rate or the patch size permits a larger critical speed. Changing the shape or scale of the dispersal kernel has, in contrast, a less consistent effect.

What is the relationship between the critical speed and the other parameters in our model? To answer this question, we turn to a mathematical analysis of the condition for population persistence.

Analysis of population persistence

Since the habitat is moving with constant speed c, we will look for a traveling pulse,

$$n_t(x) = n^*\big(\bar{x}\big) \equiv n^*(x - ct). \tag{11}$$

After substituting this solution into convolution Eq. 9, we find that

$$n^*(x - ct - c) = \int_{-\frac{L}{2}+ct}^{\frac{L}{2}+ct} k(x-y)\; f[n^*(y - ct)]\, dy. \tag{12}$$

If we change variables, so that $\bar{y} = y - ct$ and $\bar{x} = x - ct$, and shift $\bar{x}$ by c, we find that our traveling pulse must satisfy the integral equation

$$n^*(\bar{x}) = \int_{-\frac{L}{2}}^{\frac{L}{2}} k\big(\bar{x} + c - \bar{y}\big)\; f\big[n^*(\bar{y})\big]\, d\bar{y}. \tag{13}$$

For the growth functions for the Beverton–Holt curve, Eq. 5, the logistic equation, Eq. 6, and the Ricker curve, Eq. 7, $n^*(\bar{x}) = 0$ is a trivial solution. We would like to study the stability of this solution, since population persistence is equivalent to the instability of the trivial solution.

In general, the stability of a traveling pulse can be studied by adding a small perturbation, $\xi_t(x)$, to the pulse,

$$n_t(x) = n^*\big(\bar{x}\big) + \xi_t(x). \tag{14}$$

Because restriction (8) excludes Allee effects, we may linearize the right hand side of Eq. 9 about the traveling pulse to obtain

$$\xi_{t+1}(x) = \int_{-\frac{L}{2}+ct}^{\frac{L}{2}+ct} k(x-y)\; f'\big[n^*(\bar{y})\big]\, \xi_t(y)\, dy. \tag{15}$$

For the trivial solution, Eq. 15 reduces to

$$\xi_{t+1}(x) = f'(0) \int_{-\frac{L}{2}+ct}^{\frac{L}{2}+ct} k(x-y)\, \xi_t(y)\, dy. \tag{16}$$

We now write our perturbation as

$$\xi_t(x) = \lambda^t u(x - ct). \tag{17}$$

After substituting this expression into Eq. 16, we change variables, so that $\bar{y} = y - ct$ and $\bar{x} = x - ct$, and shift $\bar{x}$ by c, to obtain

$$\lambda u(\bar{x}) = f'(0) \int_{-\frac{L}{2}}^{\frac{L}{2}} k(\bar{x} + c - \bar{y})\, u(\bar{y})\, d\bar{y}. \tag{18}$$

λ is an eigenvalue of the integral operator with eigenfunction $u(\bar{x})$.

The stability of the trivial solution is determined by the dominant eigenvalue, i.e., by the eigenvalue λ with largest magnitude. The trivial solution loses stability when the magnitude of the dominant eigenvalue exceeds one.

We now restrict our domain to $(\bar{x}, \bar{y})$ that satisfy $\bar{x} \in [-L/2, L/2]$ and $\bar{y} \in [-L/2, L/2]$. If our dispersal kernel is continuous on this domain and if the interval $[-L/2, L/2]$ is finite, then the linear integral operator on the right-hand side of Eq. 18 is compact (or completely continuous). The eigenvalues of a compact linear operator form a discrete set. This set may be finite, countably infinite, or empty (Karlin 1964; Hutson and Pym 1980). Each eigenvalue is of finite multiplicity and zero is the only possible accumulation point for the eigenvalues. In general, the eigenvalues are complex. If, moreover, the kernel is positive, we may invoke Jentzsch's (1912) theorem (see also Krzemiński 1977; Horiguchi and Fukui 1996). Jentzsch's theorem is an extension of the Perron–Frobenius theorem for positive matrices to integral equations with positive kernels. The theorem guarantees the existence of a simple and positive dominant eigenvalue with positive eigenfunction. If the conditions of the theorem are satisfied, persistence is gained or lost as the dominant eigenvalue passes through $\lambda = 1$.

Continuous dispersal kernels with infinite support, such as the Laplace and Gaussian distributions, always satisfy Jentzsch's theorem for $[-L/2, L/2]$ finite. Continuous dispersal kernels with compact support may also satisfy this theorem, but only if the radius of their support is sufficiently large relative to the patch size L and speed c.

A simple, separable example

Eigenvalue problem (18) simplifies to a finite-dimensional problem in linear algebra if its kernel is separable (or degenerate). A kernel is separable (Pipkin 1991; Latore et al. 1998) if it can be written as a finite, linear combination of products of a function of x alone and a function of y alone,

$$k(x, y) = \sum_{i=1}^{N} g_i(x)\, h_i(y). \tag{19}$$

Consider, for example, the kernel

$$k(x - y) = \begin{cases} \dfrac{\omega}{2} \cos \omega(x - y), & |x - y| \le \dfrac{\pi}{2\omega}, \\ 0, & |x - y| > \dfrac{\pi}{2\omega}, \end{cases} \tag{20}$$

with finite radius of dispersal $\pi/(2\omega)$. If we assume, for convenience, that this radius of dispersal is larger than the patch size,

$$\frac{\pi}{2\omega} > L, \tag{21}$$

and that the speed c is small,

$$c < \frac{\pi}{2\omega} - L, \tag{22}$$

eigenvalue problem (18) reduces to an equation,

$$\lambda u(\bar{x}) = f'(0) \int_{-\frac{L}{2}}^{\frac{L}{2}} \frac{\omega}{2} \cos \omega(\bar{x} + c - \bar{y})\, u(\bar{y})\, d\bar{y}, \tag{23}$$

that has a kernel that is positive for all $(\bar{x}, \bar{y})$ such that $\bar{x} \in [-L/2, L/2]$ and $\bar{y} \in [-L/2, L/2]$.

The kernel is also separable, since

$$\begin{aligned} &\frac{\omega}{2} \cos \omega(\bar{x} + c - \bar{y}) \\ &= \frac{\omega}{2} \left[\cos \omega\bar{x} \cos \omega(\bar{y} - c) + \sin \omega\bar{x} \sin \omega(\bar{y} - c)\right]. \end{aligned} \tag{24}$$

Our eigenvalue problem now takes the form

$$\begin{aligned} \lambda u(\bar{x}) \;=\; & \frac{\omega R_0}{2} \left[\int_{-\frac{L}{2}}^{\frac{L}{2}} \cos \omega\,(\bar{y} - c)\, u(\bar{y})\, d\bar{y}\right] \cos \omega\bar{x} \\ & + \frac{\omega R_0}{2} \left[\int_{-\frac{L}{2}}^{\frac{L}{2}} \sin \omega\,(\bar{y} - c)\, u(\bar{y})\, d\bar{y}\right] \sin \omega\bar{x}, \end{aligned} \tag{25}$$

where $R_0 = f'(0)$.

Equation 25 implies that the eigenvector $u(\bar{x})$ can be written as a linear combination of $\cos \omega\bar{x}$ and $\sin \omega\bar{x}$,

$$u(\bar{x}) = c_1 \cos \omega\bar{x} + c_2 \sin \omega\bar{x}, \tag{26}$$

where c_1 and c_2 are constants. Inserting this expression into Eq. 25 and equating the coefficients of $\cos\,\omega\bar{x}$ and $\sin\,\omega\bar{x}$ on each side, we obtain the linear system

$$\lambda\, c_1 = a_{11}\, c_1 + a_{12}\, c_2, \tag{27a}$$

$$\lambda\, c_2 = a_{21}\, c_1 + a_{22}\, c_2, \tag{27b}$$

where

$$\begin{aligned} a_{11} &= \frac{\omega R_0}{2} \int_{-\frac{L}{2}}^{\frac{L}{2}} \cos\,\omega\big(\bar{y}-c\big)\,\cos\,\omega\bar{y}\,d\bar{y} \\ &= \frac{R_0}{4}\,(\omega L + \sin\,\omega L)\,\cos\,\omega c, \end{aligned} \tag{28a}$$

$$\begin{aligned} a_{12} &= \frac{\omega R_0}{2} \int_{-\frac{L}{2}}^{\frac{L}{2}} \cos\,\omega\big(\bar{y}-c\big)\,\sin\,\omega\bar{y}\,d\bar{y} \\ &= \frac{R_0}{4}\,(\omega L - \sin\,\omega L)\,\sin\,\omega c, \end{aligned} \tag{28b}$$

$$\begin{aligned} a_{21} &= \frac{\omega R_0}{2} \int_{-\frac{L}{2}}^{\frac{L}{2}} \sin\,\omega\big(\bar{y}-c\big)\,\cos\,\omega\bar{y}\,d\bar{y} \\ &= \frac{R_0}{4}\,(-\omega L - \sin\,\omega L)\,\sin\,\omega c, \end{aligned} \tag{28c}$$

$$\begin{aligned} a_{22} &= \frac{\omega R_0}{2} \int_{-\frac{L}{2}}^{\frac{L}{2}} \sin\,\omega\big(\bar{y}-c\big)\,\sin\,\omega\bar{y}\,d\bar{y} \\ &= \frac{R_0}{4}\,(\omega L - \sin\,\omega L)\,\cos\,\omega c. \end{aligned} \tag{28d}$$

Linear system (27) has the characteristic equation

$$\lambda^2 - \big(a_{11}+a_{22}\big)\,\lambda + \big(a_{11}a_{22} - a_{12}a_{21}\big) = 0, \tag{29}$$

which reduces to

$$\lambda^2 - \left(\frac{R_0\,\omega L}{2}\cos\,\omega c\right)\lambda + \frac{R_0^2}{16}\left(\omega^2 L^2 - \sin^2\,\omega L\right) = 0. \tag{30}$$

Separable kernel (20) is continuous and nonnegative. If conditions (21) and (22) for the patch size, radius of dispersal, and shift speed are satisfied, the kernel is positive and Jentzsch's theorem guarantees us a simple and positive dominant eigenvalue. Stability of the trivial solution is then lost through $\lambda = 1$. Setting $\lambda = 1$ allows us to determine the critical speed c^*. Thus,

$$1 - \left(\frac{R_0\,\omega L}{2}\,\cos\,\omega c^*\right) + \frac{R_0^2}{16}\left(\omega^2 L^2 - \sin^2\,\omega L\right) = 0. \tag{31}$$

The added condition

$$\frac{R_0^2}{16}\left(\omega^2 L^2 - \sin^2\,\omega L\right) < 1 \tag{32}$$

ensures that $\lambda = 1$ is, in fact, the dominant eigenvalue. The critical speed c^* occurs within just one function of Eq. 31 and, if we solve for c^*, we quickly find that

$$c^* = \frac{1}{\omega}\,\cos^{-1}\left[\frac{16 + R_0^2\left(\omega^2 L^2 - \sin^2\,\omega L\right)}{8\,R_0\,\omega L}\right], \tag{33}$$

for

$$\frac{4}{\omega L\,+\,\sin\omega L} < R_0 < R_{\max}\,. \tag{34}$$

The critical speed is zero for smaller values of R_0. The upper limit on R_0 for our analysis, $R_{\max}$, is determined by the more stringent of conditions (22), for $c = c^*$, or (32).

For separable kernel (20) and conditions (21) and (22), we can also say something about the shape of any traveling pulses. Pulse equation (13) now takes the form

$$n^*(\bar{x}) = \frac{\omega}{2}\int_{-\frac{L}{2}}^{\frac{L}{2}} \cos\,\omega\left(\bar{x}+c-\bar{y}\right)\,f\big[n^*(\bar{y})\big]\,d\bar{y}, \tag{35}$$

which, because of our separable kernel, reduces to

$$\begin{aligned} n^*(\bar{x}) \;=\; & \frac{\omega}{2}\left\{\int_{-\frac{L}{2}}^{\frac{L}{2}} \cos\,\omega\left(\bar{y}-c\right)\,f\big[n^*(\bar{y})\big]\,d\bar{y}\right\}\cos\,\omega\bar{x} \\ & + \frac{\omega}{2}\left\{\int_{-\frac{L}{2}}^{\frac{L}{2}} \sin\,\omega\left(\bar{y}-c\right)\,f\big[n^*(\bar{y})\big]\,d\bar{y}\right\}\sin\,\omega\bar{x}. \end{aligned} \tag{36}$$

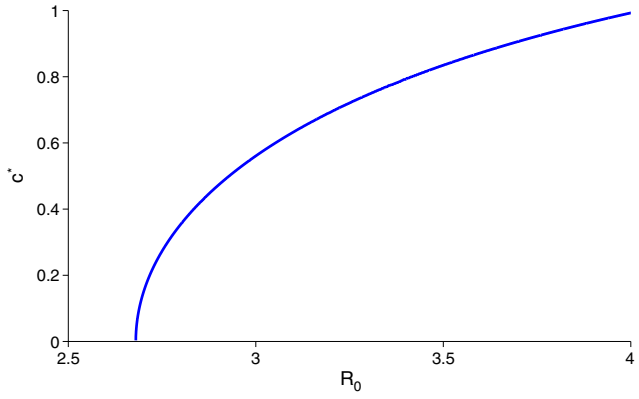

Fig. 2 A plot of the critical speed (for extinction) as a function of the net reproductive rate R_0 for a population with Beverton–Holt growth, Eq. 5, and separable kernel (20). We used critical-speed equation (33) with patch size $L = 1$ and $\omega = \pi/4$ to draw this graph. Condition (22) requires $c < 1$

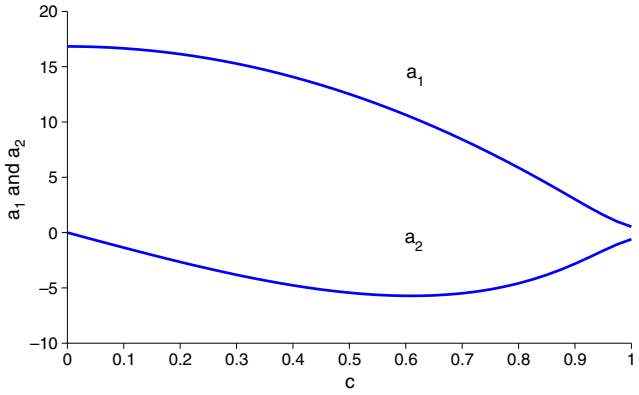

Fig. 3 Shape coefficients a_1 and a_2 of traveling pulse (37) plotted as functions of the speed c. The coefficient a_1 is proportional to the total within-patch population while a_2 introduces asymmetry into the traveling pulse. Here, $L = 1$, $R_0 = 4$, $\omega = \pi/4$, $K = 100$

It is clear from this last equation that any traveling pulse $n^*(\bar{x})$ is a linear combination of cos $\omega\bar{x}$ and sin $\omega\bar{x}$. We thus let

$$n^*(\bar{x}) = a_1 \cos \omega\bar{x} + a_2 \sin \omega\bar{x}, \tag{37}$$

with constant coefficients a_1 and a_2. After substituting this expression into Eq. 36 and equating the coefficients of cos $\omega\bar{x}$ and sin $\omega\bar{x}$ on each side, we discover that a_1 and a_2 must satisfy

$$a_1 = \frac{\omega}{2} \int_{-\frac{L}{2}}^{\frac{L}{2}} \cos \omega\left(\bar{y} - c\right) f\left(a_1 \cos \omega\bar{y} + a_2 \sin \omega\bar{y}\right) d\bar{y}\,, \tag{38a}$$

$$a_2 = \frac{\omega}{2} \int_{-\frac{L}{2}}^{\frac{L}{2}} \sin \omega\left(\bar{y} - c\right) f\left(a_1 \cos \omega\bar{y} + a_2 \sin \omega\bar{y}\right) d\bar{y}\,. \tag{38b}$$

For an arbitrary growth function, solving this nonlinear system for a_1 and a_2 is hard. These two equations do, however, provide a useful numerical scheme for calculating these coefficients. Begin by guessing a_1 and a_2, evaluate the right-hand sides of the two equations, and use these values as your new best guesses of a_1 and a_2. Repeat as needed. In our next example, this iterative scheme rapidly converges to the true a_1 and a_2.

To make the above discussion concrete, we focus on a population that obeys the Beverton–Holt stock-recruitment curve, Eq. 5; that has a patch size of one, $L = 1$; and that obeys dispersal kernel (20) with a radius of dispersal of two, so that $\omega = \pi/4$. Because of condition (22), we assume that $c < 1$. We plot the critical speed c^* as a function of the net reproductive rate R_0 (see Fig. 2) using Eq. 33. (For higher speeds, the trivial equilibrium is stable and the population goes extinct.) The plotted curve increases monotonically and is concave down. Thus, as the critical speed c^* increases, a population must increase its net reproductive rate faster and faster to persist.

In Fig. 3, we use system (38) to determine and plot the shape coefficients a_1 and a_2 of traveling pulse (37) as a function of the speed c for $0 \le c \le 1$, $L = 1$, $\omega = \pi/4$, and $R_0 = 4$. For the traveling pulse, the total population within the moving patch is proportional to the parameter a_1 and we see that this coefficient decreases monotonically as the speed c increases.

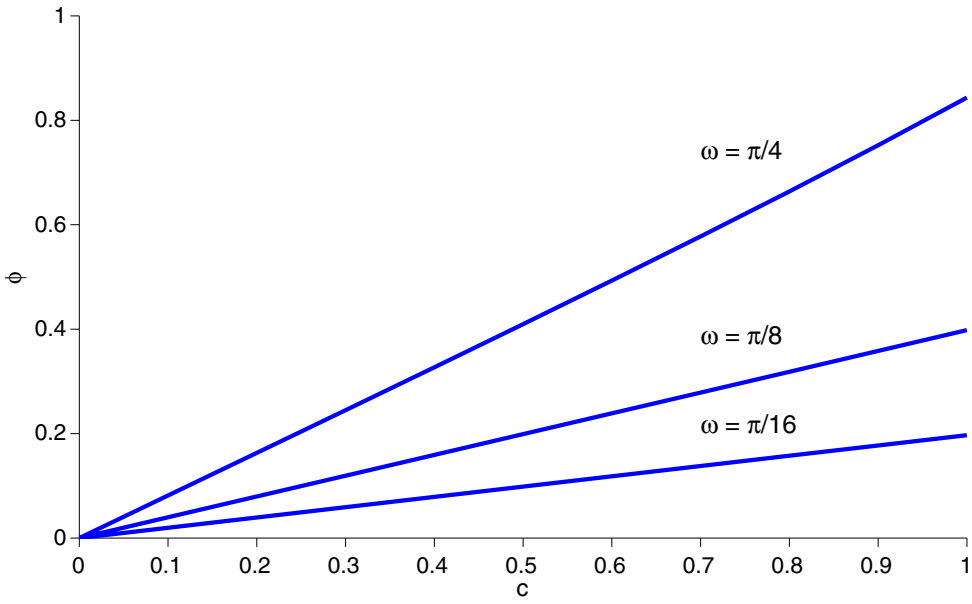

Fig. 4 Phase lag ϕ, as defined by Eq. 41, plotted as a function of the speed c. As the speed c increases, the phase lag increases more or less linearly. The phase lag was computed for $L = 1$, $R_0 = 4$, and $\omega = \pi/16, \pi/8$, and $\pi/4$

The coefficient a_2 introduces asymmetry into the pulse. To see this, we rewrite traveling pulse (37) as

$$n^*(\bar{x}) = A\,\cos\,(\omega\bar{x} + \phi) \tag{39}$$

with amplitude

$$A \equiv \sqrt{a_1^2 + a_2^2} \tag{40}$$

and phase lag

$$\phi \equiv \tan^{-1}\left(\frac{-a_2}{a_1}\right). \tag{41}$$

As c increases, the phase lag (see Fig. 4) increases and the distribution of organisms within the habitat is increasingly asymmetric: individuals pile up near the lagging edge of the patch.

Numerical methods

Although separable kernels are tractable, they are also relatively rare. For most kernels, we need numerical methods.

The most useful numeric procedures for analyzing eigenvalue problem (18) all start with the Nyström method (Delves and Walsh 1974; Press et al. 1992). That is, these procedures all begin by discretizing the integral using a quadrature rule.

The simplest quadrature rule is the repeated trapezoidal rule, which reduces Eq. 18 to

$$\lambda\,u(\bar{x}_i) = f'(0)\,\frac{\Delta\bar{x}}{2}\sum_{j=1}^{N-1}\Big[k(\bar{x}_i + c - \bar{y}_j)\,u(\bar{y}_j) + k(\bar{x}_i + c - \bar{y}_{j+1})\,u(\bar{y}_{j+1})\Big] \tag{42}$$

for $i = 1, \ldots, N$. Here, the domain of integration is discretized into $N-1$ equal subintervals of length $\Delta\bar{x} = L/(N-1)$. The variables $\bar{x}$ and $\bar{y}$ in Eq. 18 are each replaced by grid points that range from $-L/2$ to $L/2$ in units of $\Delta\bar{x}$ and that are labeled $\bar{x}_i$ and $\bar{y}_j$. If we let $c_i = u(\bar{x}_i)$,

$$A_{i1} = \frac{\Delta\bar{x}}{2}\,k(\bar{x}_i + c - \bar{y}_1), \tag{43a}$$

$$A_{ij} = \Delta\bar{x}\,k(\bar{x}_i + c - \bar{y}_j),\ 2 \le j \le N-1, \tag{43b}$$

$$A_{iN} = \frac{\Delta\bar{x}}{2}\,k(\bar{x}_i + c - \bar{y}_N), \tag{43c}$$

we now obtain the finite-dimensional linear system

$$\lambda\,c_i = f'(0)\sum_{j=1}^{N} A_{ij}\,c_j, \tag{44}$$

where $i = 1, \ldots, N$.

We can now analyze linear system (44) in one of two ways. The first approach starts by determining the eigenvalues of system (44) directly. The eigenvalues may be obtained using commands such as *eigs*, *eigen*, or *spec* in computing environments such as MATLAB, R, or Scilab or by using well-known routines from numerical libraries such as *Numerical Recipes* (Press et al. 1992), LAPACK (Anderson et al. 1999), or the GNU Scientific Library (Galassi et al. 2009). These commands and routines commonly balance a matrix, reduce the balanced matrix to Hessenberg form, and find the eigenvalues of the Hessenberg matrix using a QR algorithm. (See Press et al. 1992 for details.) Choose the dominant eigenvalue. Since this eigenvalue depends continuously on the parameters of the model, one can find the critical value for a parameter, such as c, corresponding to an important root, such as $\lambda = 1$, using a standard root-finding algorithm, such as the method of bisection or Brent's method (Brent 1973; Press et al. 1992).

As an alternative, set λ, in linear system (44), equal to one; use an efficient algorithm, such as LU decomposition (Press et al. 1992), to evaluate the determinant of the system; and use a numerical root finder to find the value of a chosen parameter that makes the determinant zero. This approach has the advantage of being simpler to implement from scratch, but has the disadvantage that you are not guaranteed that $\lambda = 1$ is always the dominant eigenvalue.

Using these numerical methods, we extended Fig. 2 for values of R_0 ($R_0 = f'(0)$ for growth function (5)) and c^* that violate smallness condition (22) (for $c = c^*$). The resulting curve (not shown) continues as before; it is monotonically increasing and concave down. A plot of the critical speed c^* as a function of the radius of dispersal, $\pi/(2\omega)$, for separable kernel (20) and $L = 1$ and $R_0 = 4$, in turn, shows (see Fig. 5) that c^* increases with the dispersal radius when the radius is small, but decreases when the radius is large. When the radius is small, most propagules land within the old patch and increasing the radius helps propagules colonize the newly avaiable habitat in front of the old patch. In contrast, for large radii, most propagules already land outside of the old patch; increasing the radius now leads to overdispersal as more individuals land behind the old patch or in front of the newly available habitat.

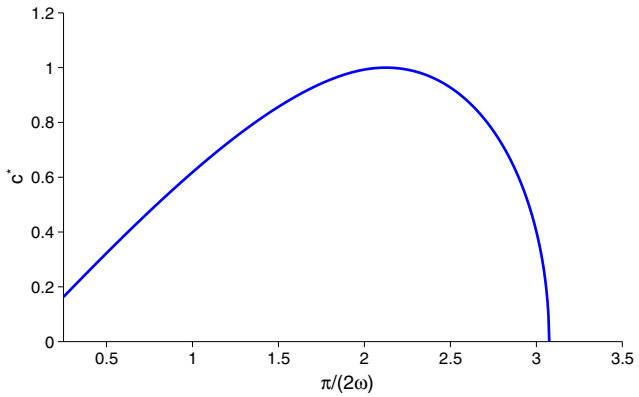

Fig. 5 A plot of the critical speed as a function of the dispersal radius $\pi/2\omega$ for separable kernel (20). The eigenvalue problem, Eq. 18 with kernel (20), was discretized using Nyström's method for $L = 1$ and $R_0 = 4$. For each radius of dispersal, we used a root finder (the method of bisection) with tolerance 10^{-8} to determine the critical speed c^* that made the dominant eigenvalue equal to 1

The above numerical methods also allow us to determine the critical speed for kernels that are not separable. We will see examples of this in the next section.

Application

Fender's blue butterfly (*I. icarioides fenderi*) is endemic to the Willamette Valley of Oregon and is listed as endangered by the US Fish and Wildlife Service (2000). This subspecies is, in many ways, poorly suited to our model: it is a habitat specialist, is not vagile, and does not disperse passively. (We will address these issues towards the end of this section.) Populations are, however, univoltine and do live in either isolated patches or in small, isolated clusters of patches (Schultz 1998; Crone and Schultz 2003; Schultz et al. 2003). In addition, we found good data regarding the critical patch size, growth, and dispersal of this butterfly.

The butterfly is restricted to prairie fragments that contain Kincaid's lupine (*Lupinus sulphureus* ssp. *kincaidii*) and other larval food plants (Schultz et al. 2003). Prairie has all but disappeared from the Willamette Valley because of the termination of annual burning by Kalapuya Indians (Wilson et al. 2003). This change in the historical fire regime allowed shrubs and trees to invade and shade out low-growing prairie species. Schultz and Crone (1998) recommended controlled burns as a means of restoring Fender's blue butterfly habitat. Since wildfires are expected to increase with global warming (Westerling et al. 2006), we believe that global warming could have an effect on the distribution of prairie species such as Kincaid's lupine and Fender's blue butterfly.

The sizes of *I. icarioides fenderi* habitat patches vary from "quite small" (less than 2 ha) to over 50 ha (Schultz et al. 2003, Figure 5). (Small patches often belong to small, isolated clusters.) Crone and Schultz (2003) estimated the minimum patch size for butterfly persistence to be 6 ha. To illustrate the effects of habitat shift, we will consider a patch of 25 ha, a size substantially larger than the estimated minimum patch size. Since we are working in one dimension, we will also assume that our 25 ha patch is square, with a width of 0.5 km.

Fender's blue butterflies display interesting movement patterns. Adult butterflies tend to stay within lupine patches, but occasionally wander out of these patches. Diffusion rates outside of lupine patches are many times greater than those inside lupine patches (Schultz 1998, Table 2). In addition (Schultz and Crone 2001; Crone and Schultz 2008), butterflies exhibit "an intriguing and distinctive looping behavior" at patch boundaries so that movement may, in fact, be a biased, correlated random walk (Turchin 1998), with bias towards habitat patches. These behaviors violate the assumptions underlying our use of a simple difference kernel, that dispersal is homogeneous and isotropic.

Even so, because our goals in this paper are exploratory rather than prescriptive, we will follow Clark (1998) and consider the exponential power distribution

$$k(x-y) = \frac{\beta}{2\alpha\Gamma(1/\beta)} \exp\left[-\left(\frac{|x-y|}{\alpha}\right)^{\beta}\right] \tag{45}$$

for dispersal, where Γ denotes the gamma function and α and β are positive scale and shape parameters. β controls the kurtosis of the kernel: for $\beta < 2$, the kernel is leptokurtic; for $\beta > 2$, it is platykurtic. For fixed β, α can then be estimated from the mean (absolute) deviation δ_1 since

$$\delta_1 = \frac{\alpha\Gamma(2/\beta)}{\Gamma(1/\beta)}. \tag{46}$$

For the mean deviation, we used Schultz's (1998, Table 2) estimate of the net lifetime movement distance for females within lupine of 0.4 km.

Figure 6 shows the critical speed c^* (for extinction) as a function of the net reproductive rate R_0 for a leptokurtic dispersal kernel ($\beta = 1$) and a platykurtic dispersal kernel ($\beta = 8$). We determined the critical speeds using eigenvalue equation (18) and the numerical methods in the "Numerical methods" section for $R_0 = f'(0)$, size $L = 0.5$ km, and mean deviation $\delta_1 = 0.4$ km. Butterflies with the leptokurtic kernel do

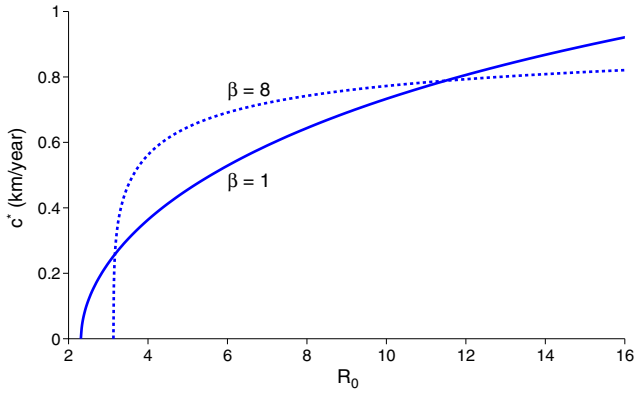

Fig. 6 Plots of the critical speed c^* as a function of the net reproductive rate R_0 for a leptokurtic and a platykurtic example of exponential power distribution (45). The solid curve is for a leptokurtic kernel ($\beta = 1$); the dot-dashed curve is for a platykurtic kernel ($\beta = 8$). The two curves were computed for mean (absolute) deviation $\delta_1 = 0.4$ km and patch width $L = 0.5$ km. For each net reproductive rate (and kernel), we used a root finder (the method of bisection) with tolerance 10^{-8} to determine the critical speed c^* that made the dominant eigenvalue of linear system (44) (as found in MATLAB) equal to 1. The effect of kurtosis on the critical speed c^* was different at small, medium, and large values of R_0

better at low and high levels of R_0 (i.e., for lower and higher speeds) while butterflies with the platykurtic kernel cope better at intermediate levels of R_0. This is consistent with the fact that the leptokurtic distribution has more probability in the center peak and in the tails (i.e., for small and large distances) while the platykurtic distribution has more probability in the shoulders.

Schultz and Hammond (2003) surveyed Fender's blue butterfly populations across the range of the subspecies and measured growth rates between 0.99 to 2.66 (see their Table 2). The high values of R_0 in Fig. 6 suggest that most extant populations of Fender's blue butterfly would do poorly with even small amounts of range shift.

The above model, as previously stated, ignores the fact that Fender's blue butterfly is a habitat specialist whose movement is strongly affected by the presence of its host plant, Kincaid's lupine, a long-lived perennial (Wilson et al. 2003). We can construct a more realistic model at the expense of simplicity. Dwyer and Morris (2006) have considered integrodifference equations, built around consumer–resource models, that include resource-dependent dispersal. One can also construct such models for Fender's blue butterfly and Kincaid's lupine.

Discrete-time consumer–resource models often take the form of host–parasitoid models. For these models, the exact order of events is extremely important (May et al. 1981; Kang et al. 2008). In the case of Fender's blue butterfly, adult females lay their eggs on appropriate host plants, plants not overgrown or shaded by taller plants, from May to June (Schultz et al. 2003). Newly hatched larvae feed for a short time, but then enter diapause until February or March. Most feeding thus takes place after the host has set seed. Larvae spend most of their time on the food plant; they seldom crawl to the ground (due, perhaps, to a large, predaceous tiger beetle) (Schultz et al. 2003). For convenience, we will assume that larvae feed only on the plant on which they were oviposited.

A more detailed model for the butterfly–lupine system might thus take the form

$$R_{t+1}(x) = \sigma\, f\big(x, R_t(x), C_t(x)\big) R_t(x) + \lambda \int_{-\frac{L}{2}+ct}^{\frac{L}{2}+ct} k(x-y)\, R_t(y)\, g\big(R_t(y)\big)\, dy\,, \quad (47a)$$

$$C_{t+1}(x) = \gamma\, \sigma \left[1 - f\big(x, R_t(x), C_t(x)\big)\right] R_t(x)\,. \quad (47b)$$

Here, $R_t(x)$ is the density of the lupine population (the resource) before reproduction, $C_t(x)$ is the density of the feeding larvae, σ is the survivorship of adult plants in the absence of consumers, λ is the number of offspring per adult plant in the absence of density dependence, γ is a factor that accounts for the conversion of consumed lupines into butterflies, $k(x-y)$ is the dispersal kernel for the lupine, $g(R_t)$ accounts for density dependence in lupine reproduction, and $f(x, R_t(x), C_t(x))$ is the fraction of adult lupine that survive herbivory. As before, we assume that all reproduction takes place in a patch of size L moving with constant speed c.

The fraction of lupine that survive herbivory ultimately depends on the density and spatial distribution of butterfly eggs. We may thus write

$$f(x, R_t(x), C_t(x)) = \begin{cases} \exp\left[-a \int_{-\frac{L}{2}+ct}^{\frac{L}{2}+ct} h\big(x-y, R_t(y)\big)\, C_t(y)\, dy\right], & x \in \left[-\frac{L}{2}+ct, \frac{L}{2}+ct\right] \\ 1, & x \notin \left[-\frac{L}{2}+ct, \frac{L}{2}+ct\right]. \end{cases} \quad (48)$$

Here, a is the area of discovery (Nicholson 1933) and $h(x-y, R_t(y))$ is a dispersal kernel for the butterfly. This kernel now depends on the distribution of host plants as well as on distance. (See Dwyer and Morris (2006) for examples of resource-dependent kernels and for other models.)

The analysis of system (47) is beyond the scope of this paper, but this example does show how one can extend our basic approach to include more biology. This example also highlights the fact that a species' ability to keep pace with range shifts may, in fact, depend on the dispersal ability of its host.

Discussion

All species have limits to how frequently and how far they disperse. If these limits are severe, climate change can take a heavy toll. In the "Model" section, we introduced a simple model for population growth on a shifting domain. We showed (see Fig. 1b) that a rapid, climate-induced, shifting species range can cause a population to die out. Even if the population persists (see Fig. 1a), it may be greatly reduced. Approaches that neglect dispersal, such as bioclimate envelope models, can overestimate the ability of species to survive in the presence of climate change.

For our model, the speed of the range shift determines the toll on the population. For a given growth function, dispersal kernel, and patch size, there is a critical speed beyond which the population cannot survive. In the "Analysis of population persistence" section, we related population persistence to a simple (integral equation) eigenvalue problem. In "A simple, separable example" section, we determined the critical speed for a simple separable kernel analytically . In Section "Numerical methods", we showed how to determine the critical speed for general dispersal kernels numerically. Other critical values, such as critical patch size and critical growth rate, can also be determined numerically.

Larger growth rates and patch sizes (graph not shown) increase population persistence. Changing the shape or scale of a dispersal kernel has a less consistent effect (see Figs. 5 and 6). Since a population's vulnerability to climate change displays a complicated relationship to its dispersal behavior, we encourage ecologists to use detailed dispersal information in managing populations for conservation. Integrodifference equation are especially useful in this regard since they are built around dispersal kernels and can accommodate varied dispersal mechanisms (Neubert et al. 1995; Neubert and Parker 2004).

In this paper, we started with the simplest reasonable model: we constructed and analyzed a deterministic model with discrete, nonoverlapping generations; compensatory growth; and homogeneous and isotropic dispersal. These assumptions can be relaxed. Instead of a compensatory (Beverton–Holt) growth function, we can easily imagine using growth functions with overcompensation, such as the logistic curve or the Ricker curve. With overcompensation, we expect traveling time-periodic or chaotic pulses. Another alternative is to use a growth function with critical depensation or a strong Allee effect (e.g., Wang et al. 2002; Taylor and Hastings 2005). Our model might then exhibit bistability and dangerous fold bifurcations. Integrodifference equations have also been extended to accommodate time-periodic, stochastic, density-dependent, and resource-dependent growth and dispersal (Neubert et al. 2000; Kot et al. 2004; Hastings et al. 2005; Dwyer and Morris 2006; Lutscher 2008) and age and stage structure (Neubert and Caswell 2000). We hope to incorporate these effects into range-shift models in the future.

Acknowledgements MK acknowledges Mark A. Lewis and Michael G. Neubert for stimulating and helpful discussions that helped inspire and further this research. We are grateful to the reviewers for their helpful comments.

References

Allee WC (1938) The social life of animals. Norton, New York

Anderson E, Bai Z, Bischof C, Blackford S, Demmel J, Dongarra J, Croz JD, Greenbaum A, Hammarling S, McKenney A, Sorensen D (1999) LAPACK user's guide. Society for Industrial and Applied Mathematics, Philadelphia

Bakkenes M, Alkemade JRM, Ihle F, Leemans R, Latour JB (2002) Assessing effects of forecasted climate change on the diversity and distribution of European higher plants for 2050. Glob Chang Biol 8:390–407

Berestycki H, Diekmann O, Nagelkerke CJ, Zegeling PA (2009) Can a species keep pace with a shifting climate? Bull Math Biol 71:399–429

Beverton RJH, Holt SJ (1957) On the dynamics of exploited fish populations. Her Majesty's Stationery Office, London

Box EO (1981) Macroclimate and Plant Forms: an introduction to predictive modeling in phytogeography. Dr. W. Junk, The Hague

Brent RP (1973) Algorithms for minimization without derivatives. Prentice-Hall, Inc., Englewood Cliffs

Cantrell RS, Cosner C (2003) Spatial ecology via reaction-diffusion equations. J. Wiley, Chichester

Clark JS (1998) Why trees migrate so fast: confronting theory with dispersal biology and the paleorecord. Am Nat 152: 204–224

Crone EE, Schultz CB (2003) Movement behavior and minimum patch size for butterfly population persistence. In: Boggs CL, Watt WB, Ehrlich PR (eds) Butterflies: ecology and

evolution taking flight. University of Chicago Press, Chicago, pp 561–576
Crone EE, Schultz CB (2008) Old models explain new observations of butterfly movement at patch edges. Ecology 89:2061–2067
Delves LM, Walsh J (1974) Numerical solution of integral equations. Clarendon Press, Oxford
Dwyer G, Morris WF (2006) Resource-dependent dispersal and the speed of biological invasions. Am Nat 167:165–176
Fagan WF, Lewis M, Neubert MG, Aumann C, Apple JL, Bishop JG (2005) When can herbivores slow or reverse the spread of an invading plant? A test case from Mount St. Helens. Am Nat 166:669–685
Fisher RA (1937) The wave of advance of advantageous genes. Ann Eugen 7:355–369
Galassi M, Davies J, Theiler J, Gough B, Jungman G, Aiken P, Booth M, Rossi F (2009) GNU scientific library: reference manual. Network Theory Ltd., Bristol
Gaston KJ (2003) The structure and dynamics of geographic ranges. Oxford University Press, Oxford
Guisan A, Thuiller W (2005) Predicting species distribution: offering more than simple habitat models. Ecol Lett 8: 993–1009
Hart DR, Gardner RH (1997) A spatial model for the spread of invading organisms subject to competition. J Math Biol 35:935–948
Hastings A, Higgins K (1994) Persistence of transients in spatially structured ecological models. Science 263:1133–1136
Hastings A, Cuddington K, Davies KF, Dugaw CJ, Elmendorf S, Freestone A, Harrison S, Holland M, Lambrinos J, Malvadkar U, Melbourne BA, Moore K, Taylor C, Thomson D (2005) The spatial spread of invasions: new developments in theory and evidence. Ecol Lett 8:91–101
Horiguchi T, Fukui Y (1996) A variation of the Jentzsch theorem for a symmetric integral kernel and its application. Interdiscip Inf Sci 2:139–144
Hughes L (2000) Biological consequences of global warming: is the signal already apparent? Trends Ecol Evol 15:56–61
Hutson V, Pym JS (1980) Applications of functional analysis and operator theory. Academic Press, London
IPCC (2007) Climate change 2007: synthesis report. Contribution of working groups I, II and III to the fourth assessment report of the intergovernmental panel on climate change. Core Writing Team and Pachauri, R. K. and Reisinger, A., IPCC, Geneva
Jeffree CE, Jeffree EP (1996) Redistribution of the potential geographical ranges of mistletoe and Colorado beetle in Europe in response to the temperature component of climate change. Funct Ecol 10:562–577
Jentzsch R (1912) Über integralgleichungen mit positivem kern. J Reine Angew Math 141:235–244
Kadmon R, Farber O, Danin A (2003) A systematic analysis of factors affecting the performance of climatic envelope models. Ecol Appl 13:853–867
Kang Y, Armbruster D, Kuang Y (2008) Dynamics of a plant–herbivore model. J Biol Dyn 2:89–101
Kareiva P (1990) Population dynamics in spatially complex environments: theory and data. Philos Trans: Biol Sci 330: 175–190
Karlin S (1964) The existence of eigenvalues for integral operators. Trans Am Math Soc 113:1–17
Keeling M (1999) Spatial models of interacting populations. In: McGlade JM (ed) Advanced ecological theory: principles and applications. Blackwell Science, Malden, pp 64–99
Kot M (1992) Discrete-time travelling waves: ecological examples. J Math Biol 30:413–436
Kot M, Schaffer WM (1986) Discrete-time growth-dispersal models. Math Biosci 80:109–136
Kot M, Lewis MA, Van Den Driessche P (1996) Dispersal data and the spread of invading organisms. Ecology 77:2027–2042
Kot M, Medlock J, Reluga T, Walton DB (2004) Stochasticity, invasions, and branching random walks. Theor Popul Biol 66:175–184
Krzemiński S (1977) Comment on 'A simple proof of the Perron–Frobenius theorem for positive symmetric matrices'. J Phys A Math Gen 10:1437–1438
Latore J, Gould P, Mortimer AM (1998) Spatial dynamics and critical patch size of annual plant populations. J Theor Biol 190:277–285
Latore J, Gould P, Mortimer AM (1999) Effects of habitat heterogeneity and dispersal strategies on population persistence in annual plants. Ecol Model 123:127–139
Letcher TM (2009) Climate change: observed impacts on planet Earth. Elsevier, Amsterdam
Lewis MA (1997) Variability, patchiness, and jump dispersal in the spread of an invading population. In: Tilman D, Kareiva P (eds) Spatial ecology: the role of space in population dynamics and interspecific interactions. Princeton University Press, Princeton, pp 46–69
Lewis MA, Neubert MG, Caswell H, Clark JS, Shea K (2006) A guide to calculating discrete-time invasion rates from data. In: Cadotte MW, McMahon SM, Fukami T (eds) Conceptual ecology and invasions biology: reciprocal approaches to nature. Springer, Dordrecht, pp 169–192
Lockwood DR, Hastings A, Botsford LW (2002) The effects of dispersal patterns on marine reserves: does the tail wag the dog? Theor Popul Biol 61:297–309
Lovejoy TE, Hannah L (2005) Climate change and biodiversity. Yale University Press, New Haven
Lui R (1983) Existence and stability of travelling wave solutions of a nonlinear integral operator. J Math Biol 16:199–220
Lutscher F (2008) Density-dependent dispersal in integrodifference equations. J Math Biol 56:499–524
May RM (1973) On relationships among various types of population models. Am Nat 107:46–57
May RM, Hassell MP, Anderson RM, Tonkyn DW (1981) Density dependence in host–parasitoid models. J Anim Ecol 50:855– 865
Maynard Smith J (1968) Mathematical ideas in biology. Cambridge University Press, London
McCarty JP (2001) Ecological consequences of recent climate change. Conserv Biol 15:320–331
Mitikka V, Heikkinen RK, Luoto M, Araújo MB, Saarinen K, Pöyry J, Fronzek S (2008) Predicting range expansion of the map butterfly in Northern Europe using bioclimatic models. Biodivers Conserv 17:623–641
Neubert MG, Caswell H (2000) Demography and dispersal: calculation and sensitivity analysis of invasion speed for structured populations. Ecology 81:1613–1628
Neubert MG, Parker IM (2004) Projecting rates of spread for invasive species. Risk Anal 24:817–831
Neubert MG, Kot M, Lewis MA (1995) Dispersal and pattern formation in a discrete-time predator-prey model. Theor Popul Biol 48:7–43
Neubert MG, Kot M, Lewis MA (2000) Invasion speeds in fluctuating environments. Proc R Soc Lond B 267: 1603–1610
Nicholson AJ (1933) The balance of animal populations. J Anim Ecol 2:132–178

Okubo A (1980) Diffusion and ecological problems: mathematical models. Springer, Berlin

Osborne JL, Loxdale HD, Woiwod IP (2002) Monitoring insect dispersal: methods and approaches. In: Bullock JM, Kenward RE, Hails RS (eds) Dispersal ecology: the 42nd symposium of the British ecological society held at the University of Reading 2–5 April 2001. Blackwell Science, Malden, pp 24–49

Parmesan C (2006) Ecological and evolutionary responses to recent climate change. Annu Rev Ecol Evol Systemat 37: 637–669

Parmesan C, Ryrholm N, Stefanescu C, Hill JK, Thomas CD, Descimon H, Huntley B, Kaila L, Kullberg J, Tammaru T, Tennent WJ, Thomas JA, Warren M (1999) Poleward shifts in geographical ranges of butterfly species associated with regional warming. Nature 399:579–583

Pearson RG, Dawson TP (2003) Predicting the impacts of climate change on the distribution of species: are bioclimate envelope models useful? Glob Ecol Biogeogr 12:361–371

Pipkin AC (1991) A course on integral equations. Springer-Verlag, New York

Potapov AB, Lewis MA (2004) Climate and competition: the effect of moving range boundaries on habitat invasibility. Bull Math Biol 66:975–1008

Press WH, Teukolsky SA, Vetterling WT, Flannery BP (1992) Numerical recipes in C: the art of scientific computing. Cambridge University Press, Cambridge

Ricker WE (1954) Stock and recruitment. J Fish Res Board Can 11:559–623

Schultz CB (1998) Dispersal behavior and its implications for reserve design in a rare oregon butterfly. Conserv Biol 12: 284–292

Schultz CB, Crone EE (1998) Burning prairie to restore butterfly habitat: a modeling approach to management tradeoffs for the Fender's blue. Restor Ecol 6:244–252

Schultz CB, Crone EE (2001) Edge-mediated dispersal behavior in a prairie butterfly. Ecology 82:1879–1892

Schultz CB, Hammond PC (2003) Using population viability analysis to develop recovery criteria for endangered insects: case study of the Fender's blue butterfly. Conserv Biol 17:1372–1385

Schultz CB, Hammond PC, Wilson MV (2003) Biology of the Fender's blue butterfly (*Icaricia icarioides fenderi Macy*), an endangered species of western Oregon native prairies. Nat Areas J 23:61–71

Shigesada N, Kawasaki K (1997) Biological invasions: theory and practice. Oxford University Press, Oxford

Shigesada N, Kawasaki K (2002) Invasion and the range expansion of species: effects of long-distance dispersal. In: Bullock J, Kenward R, Hails R (eds) Dispersal ecology. Blackwell Science, Oxford, pp 350–373

Skellam JG (1951) Random dispersal in theoretical populations. Biometrika 38:196–218

Taylor CM, Hastings A (2005) Allee effects in biological invasions. Ecol Lett 8:895–908

Turchin P (1998) Quantitative analysis of movement. Sinauer Associates, Inc., Sunderland

US Fish and Wildlife Service (2000) Endangered and threatened wildlife and plants; endangered status for *Erigeron decumbens* var. *decumbens* (Willamette daisy) and Fender's blue butterfly (*Icaricia icarioides fenderi*) and threatened status for *Lupinus sulphureus ssp. kincaidii* (Kincaid's lupine). Fed Regist 65:3875–3890

Van Kirk RW, Lewis MA (1997) Integrodifference models for persistence in fragmented habitats. Bull Math Biol 59: 107–137

Van Kirk RW, Lewis MA (1999) Edge permeability and population persistence in isolated habitat patches. Nat Resour Model 12:37–64

Walther GR, Post E, Convey P, Menzel A, Parmesan C, Beebee TJC, Fromentin JM, Hoegh-Guldberg O, Bairlein F (2002) Ecological responses to recent climate change. Nature 416:389–395

Wang MH, Kot M, Neubert MG (2002) Integrodifference equations, Allee effects, and invasions. J Math Biol 44:150–168

Weinberger HF (1978) Asymptotic behavior of a model in population genetics. Lect Notes Math 648:47–96

Weinberger HF (1982) Long-time behavior of a class of biological models. SIAM J Math Anal 13:353–396

Westerling AL, Hidalgo HG, Cayan DR, Swetnam TW (2006) Warming and earlier spring increase western U.S. forest wildfire activity. Science 313:940–943

Wilson MV, Erhart T, Hammond PC, Kaye TN, Kuykendall K, Liston A, Robinson Jr AF, Schultz CB, Severns PM (2003) Biology of Kincaid's lupine(*Lupinus sulphureus ssp. kincaidii* [Smith] Phillips), a threatened species of western Oregon native prairies, USA. Nat Areas J 23:72–83